Наносистеми, наноматеріали, нанотехнології
Nanosistemi, Nanomateriali, Nanotehnologii
2022, т. 20, № 3, сс. 745–760

PACS numbers: 07.20.Fw, 64.60.Ej, 64.70.D-, 68.35.bp, 81.70.Pg, 82.60.Fa, 84.60.Ve

Express Method of Experimental Investigation of the Effect of Carbon Nanostructures on the Caloric Properties of Paraffin Wax

Yana Hlek[1], Olga Khliyeva[2], Dmytro Ivchenko[1], Mykola Lapardin[1], Viacheslav Khalak[1], and Vitaly Zhelezny[1]

[1]*Odesa National Academy of Food Technologies,*
1/3, Dvoryanska Str.,
UA-65082 Odesa, Ukraine
[2]*National University 'Odesa Maritime Academy',*
8, Didrikhson Str.,
UA-65029 Odesa, Ukraine

The rational selection of the components of thermal-storage composite materials with phase change (PCMs) based on industrial paraffin wax (PW) and carbon nanostructures (CNS) will help to improve the efficiency of the thermal-storage systems. An experimental setup of a new design for measuring the caloric properties of the composite PCMs was created. Its main advantages are simple design, low cost and the possibility of samples visualization during the experiment. The setup applying is appropriate for estimation of the expediency of further composite PCMs' studying. The objects of experimental study are as follow: industrial PW with a melting point of 53.5°C, PW containing 0.000936 $g \cdot g^{-1}$ of fullerene C_{60}, and PW containing 0.111 $g \cdot g^{-1}$ of expanded graphite (EG). The EG in PW contributes to a slight decrease in temperatures of phase-transition start and finish (0.5–2.0°C); the presence of C_{60} does not influence these parameters. The phase-transition total enthalpy for PW/EG is by 15–21% less, and for PW/C_{60} is by 7–16% higher than for PW. The EG presence contributes to decreasing the heat capacity of PW liquid phase by 10–16%; oppositely, the 7–15% increase is observed at C_{60} presence in PW. The obtained effects can be explained by both the presence of CNSs themselves and the structural changes in PW caused by CNSs. The obtained results have established the expediency of further studies of the composite PW/CNSs PCMs to confirm the obtained effects for PW/C_{60} and to find the rational content of EG in PW/EG.

Раціональний вибір компонентів композитних термоакумулювальних матеріялів (ТАМ) із фазовим переходом на основі технічного парафіну (ТП) та вуглецевих наноструктур сприятиме підвищенню ефективности термоакумуляторів. Запропоновано нову конструкцію експериментальь-

ної установки для міряння калоричних властивостей композитних ТАМ з фазовим переходом, яка вирізняється простотою конструкції, низькою вартістю та можливістю візуального спостереження за досліджуваним зразком. Застосування установки доречно для оцінювання доцільности подальшого вивчення композитних ТАМ. Об'єктами експериментального дослідження були: технічний парафін з температурою топлення у 53,5°C, парафін із вмістом 0,000936 г·г$^{-1}$ фуллерену C_{60} і парафін із вмістом 0,111 г·г$^{-1}$ терморозширеного графіту (ТРГ). Присутність ТРГ в парафіні сприяє незначному пониженню температур початку та кінця фазового переходу (0,5–2,0°C); присутність C_{60} практично не впливає на ці параметри. Повна ентальпія фазового переходу для ТП/ТРГ була на 15–21% меншою, а для ТП/C_{60} — на 7–16% вищою, ніж для ТП. Присутність ТРГ сприяє пониженню тепломісткости рідкої фази парафіну на 10–16%, присутність C_{60} — збільшенню тепломісткости на 7–15%. Одержані ефекти можуть бути пояснені як присутністю самих вуглецевих наноструктур, так і зміною структури парафіну через їхню присутність у парафіні. Показано доцільність подальших досліджень композитних ТАМ на основі парафіну та вуглецевих наноструктур задля підтвердження одержаних ефектів для PW/C_{60} і з метою пошуку раціональної концентрації ТРГ у ТП/ТРГ.

Key words: thermal storage, industrial paraffin wax, fullerene C_{60}, expanded graphite, specific isobaric heat capacity, total phase-transition enthalpy.

Ключові слова: термоакумулювання, технічний парафін, фуллерен C_{60}, терморозширений графіт, питома ізобарна тепломісткість, повна ентальпія фазового переходу.

(Received 24 January, 2022; in revised form, 27 January, 2022)

1. INTRODUCTION

Thermal energy storage (TES) systems with phase change materials (PCMs) have drawn considerable attention from scientists last decade. TES systems with PCMs can absorb/release a large amount of heat within the operating temperature range due to the phase transition. Consequently, such systems can help address the mismatch between the energy incoming into the heat power systems and heat-energy output demand. Eliminating in/out energy mismatch is of prime importance to improve renewable energy utilization rate.

TES systems based on paraffin wax (PW) have great prospects for heating and hot water supply systems [1]. However, the low thermal conductivity of PW restricts its thermal performance and limits its large-scale applications. Adding a suitable proportion of high thermal conductivity components into the PW can enhance the heat transfer rate, and thus, improve the thermal efficiency of the whole TES [2, 3].

Expanded graphite (EG) and fullerene C_{60} are promising CNS for thermal conductivity enhancement. EG is highly thermally conductive and has a porous structure, making it an ideal candidate for the shape stabilization of PCMs [2]. At the same time, the use of C_{60} as a component of PCM is of aroused interest, since it was shown that a small portion of C_{60} significantly increases the thermal conductivity of PW [4]. In addition, C_{60} is contained in saturated hydrocarbons of high molecular mass (paraffin) in dissolved state simultaneously as small nanoparticles and large molecules without aggregation and precipitation [5].

There are quite a lot of papers dedicated to the measurement of the composite PCMs thermal conductivity but there are no studies of its caloric properties. For example, in Ref. [6], the effect of EG granules size on the structure and thermal conductivity of PW/EG was investigated. A thermal conductivity enhancement of up to 1695% compared with the PW was observed for the PW containing large EG particles *vs.* 340% for the fine EG particles. Regardless of the obtained excellent effect on thermal conductivity, the effect on the phase transition heat has not been studied. At the same time, the conclusion on the expediency of the studied PCMs in the industry can be obtained only after its thermal storage capacity studying.

Analysis of many studies shows that the presence of the solid components in composite PCMs with phase transition contribute to reducing their specific heat capacity and phase transition enthalpy (the latent heat of fusion) [2, 7, 8, 9, 10]. This effect is undesirable for TES systems. For example, in Ref. [7], it was shown that latent heat of fusion of the composite PCM with PW (92.2, 90.0, and 88.7 vol.% of PW) decreases with EG volume fraction increase. In Ref. [8], the EG (15 wt.%) was applied to support *n*-eicosane (paraffin C20) via vacuum impregnation. The DSC analysis indicated that the *n*-eicosane/EG has latent heat values of 199.4 $J \cdot g^{-1}$ for melting and 199.2 $J \cdot g^{-1}$ for freezing, exhibiting a large thermal storage capacity. The thermal conductivity of the composite with 15 wt.% of EG is 14.4 times more than that of pure *n*-eicosane, and the heating and cooling curves confirmed that the EG has substantially improved the thermal transfer rate of samples. Although the latent heat values for composite PCMs were obtained, it was not noted how these values decreased compared with the pure *n*-eicosane. The effect of the 2 wt.%, 4 wt.%, and 6 wt.% of EG (FireCarb TEG-315—*A*-type and FireCarb TEG-160—*B*-type) on the total heat storage capacity due to the phase transition of PW (melting temperature range of 53–57°C) were studied in [9]. The total heat storage capacity (differential scanning calorimeter) for PW is 144 $J \cdot g^{-1}$ vs 136 $J \cdot g^{-1}$ for *A*-type PW/EG. At the same time, the total heat storage capacity for *B*-type PW/EG varies between 140 and 154 $J \cdot g^{-1}$.

This result is very promising for industrial applications.

The express study of the effect of various PCM components on caloric properties of promising composite PCMs is greatly important during their full-scale studying. The purpose of this study was to create the setup for express analysis of the caloric properties of composite PCMs and to investigate the effect of CNSs in PW on its specific isobaric heat capacity and the phase transition total enthalpy to analyse the expediency of application of the considered composite PCMs in TES systems. A rational selection of the PCMs components will contribute to an increase in the reaction rate of the system to thermal influences and, thus, to an increase of the overall efficiency of the TES systems [11].

2. MATERIALS AND OBJECTS OF STUDY

The following materials were used to prepare the composite PCMs:

— paraffin wax (PW) (industrial grade T-3, melting temperature 53.5°C, produced in Poland);

— fullerene C_{60} (purchased from Suzhou Dade Carbon Nanotechnology Co., Ltd., China, CAS# 99685-96-8), purity 0.995 $g \cdot g^{-1}$;

— expanded graphite (highly conductive expanded graphite powder GFG200, supplier the SGL Sigratherm, Germany, purity not less than 95 wt.%, D_{50} determined by sieve analysis 200 μm, powder bulk density 100 $g \cdot l^{-1}$).

The technique of PCM preparation was based on pristine EG mixing with moulted PW (70–75°C) and mechanical stirring of the components. No previous treatment of components was implemented. A rapid separation into pure PW and PW containing EG with a clear interface was observed several hours after preparing the composite PCM. It is assumed that stable and almost fully filled by PW structure of EG has been obtained in the precipitated layer. After crystallization of the PW/EG, the upper pure PW was carefully removed and weighed. The required quantity of the components was measured using the Model GR 300 electronic balance with the instrument uncertainty of 0.5 mg.

The first step of the composite PCMs preparation containing C_{60} consists of C_{60} mixing with molten PW, mechanical stirring, and sonication for 2 hours using an ultrasonic generator UZG 13-0.1/22 (frequency 22 kHz, power 0.1 kW). During ultrasonic treatment, the temperature was maintained at about 65 ± 5°C. During the second step, the composite PCM containing C_{60} was kept for 5 days in the liquid phase at the temperature of about 70°C. This is necessary because it takes considerable time to reach the saturation equilibrium, namely, from several hours to several days. Sonication not only accelerates C_{60} dissolution but also can contribute to the formation

a *b* *c*

Fig. 1. The pictures of the composite PCM samples: *a*—pure PW; *b*—PW containing 0.000936 $g \cdot g^{-1}$ of C_{60}; *c*—PW containing the 0.111 $g \cdot g^{-1}$ of EG.

of supersaturated fullerene solutions with its further crystallization [5]. The obtained solution was considered supersaturated, since during the following 5 days precipitation of C_{60} crystals was observed. The precipitate with C_{60} crystals was removed after PW/C_{60} crystallization. The precipitate was weighed, washed repeatedly by *n*-pentane to remove PW (C_{60} has very low solubility in n-pentane 0.005 $mg \cdot ml^{-1}$ at 20°C [12]), filtered through a paper filter and weighed. Thus, the saturated solution of C_{60} in PW was obtained and the saturation mass fraction of C_{60} at 65–70°C was determined.

Thus, three PCMs were used in the further experiments:

— pure PW (shown as PW in the figures and text);

— PW containing the 0.000936 $g \cdot g^{-1}$ of fullerene C_{60} (shown as PW/C_{60} in the figures and text);

— PW containing the 0.111 $g \cdot g^{-1}$ of EG (shown as PW/EG in the figures and text).

The pictures of the PCM samples (in form of pellets with diameter 25 ± 0.2 mm and thickness 4.0–6.5 mm) are presented in Fig. 1.

3. EXPERIMENTAL SETUP AND TECHNIQUE OF EXPERIMENT

The measurement of the phase transition total enthalpy and specific isobaric heat capacity of the composite PCM samples was performed by the method of monotonic heating in the calorimeter of the variable temperature. The schematic diagram of the experimental setup is presented in Fig. 2.

To minimize the heat losses from the measuring cell, the following design approaches were used: vacuum-degassing the system under the vacuum glass cover up to 0.05 mm Hg (6.67 Pa); mounting the aluminium foil screen *10*; installation of the measuring cell *8* on a metal plate *2* using three thin Teflon pins.

The calorimetric heater *7* made of a constantan wire (0.15 mm in diameter and 4.2 m in length) was installed in the middle of the measuring cell. The electrical resistance of the heater was 125 Ohm. The heater *7* was installed in such a way as to form a uniform tem-

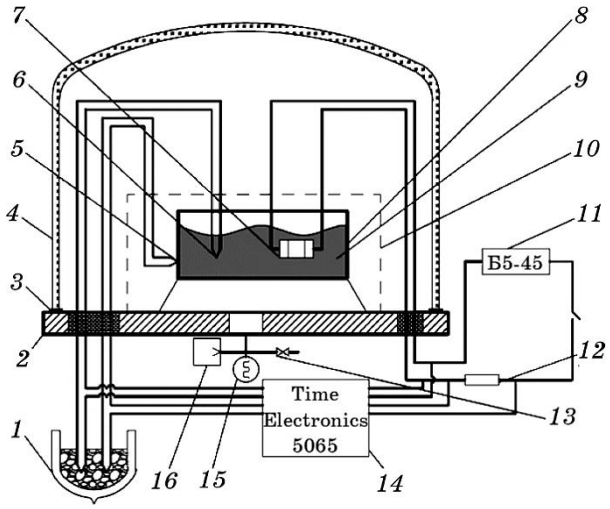

Fig. 2. Schematic diagram of the experimental setup: *1* is the Dewar vessel with $t = 0$°C; *2* is the metal plate; *3* is the vacuum seal; *4* is vacuum glass cover; *5*, *6* are the thermocouples; *7* is the electric heater; *8* is the measuring cell; *9* is the test sample; *11* is the regulated power supply; *12* is the standard resistor; *13* is the air-admission valve; *14* is the multimeter; *15* is the thermocouple vacuum transducer; *16* is the vacuum pump.

perature field during heating. The regulated power supply *11* was applied for electricity supplying of the colorimetric heater *7*. Electric current parameters of the calorimetric heater *7* were measured by the multimeter *14* by realizing the compensation method with the reference resistance coil *12*. The power of the heater *7* during the experiment was 1.786 ± 0.002 W. The temperatures of the sample and the surface of the cell were measured with a step of 6 seconds using the absolute thermocouples *6* and *5*, correspondingly.

Preparation for the experiment contained the following steps: weighing the PCM sample in the measuring cell *8* (the sample had to cover the heater); installing the glass cover *4* on the metal plate *2* and turning on the vacuum system; turning on the heater *7* when the pressure reaches 0.05 mm Hg. Next, the readings of the thermocouples *5* and *6* and electric current parameters on the heater were recorded every 6 seconds until the thermocouple *5* readings reached approx. 80°C (heating mode). The heater was turned off and the readings of the thermocouples *5* and *6* were recorded until the thermocouple *5* readings reached approx. 35°C (cooling mode). The test was performed twice for each sample. Masses of the samples were the following: 7.9900 g for PW, 7.8606 g for PW/C_{60}, and 7.2118 g for PW/EG.

The measurement of heat loss at different temperatures of the

cell wall (readings of thermocouple *5*) has been performed. The time-constant power of the heater *7* that ensured the constancy of the thermocouple *5* readings was determined in the multiplied experiment (Fig. 3). The obtained temperature dependence of heat loss was fitted by Eq. (1):

$$P_{loss} = -0.00058047t_5^2 + 0.086109t_5 - 1.8449, \quad (1)$$

where t_5 is the temperature of the measuring cell wall (readings of the thermocouple *5*) [°C].

Moreover, the calorimeter heat capacity (the energy needed to increase the temperature of the calorimeter elements, namely, measuring cell *8*, thermocouples *5* and *6*, heater *7*, per one °C) was calculated. In the range of the experiment temperatures, the calorimeter heat capacity was assumed constant: $A = 8.25036$ J·K^{-1}.

The heat supplied to the studied PCM sample during its heating was calculated by Eq. (2):

$$Q = P\Delta\tau - P_{loss}\Delta\tau - A\Delta t, \quad (2)$$

where P is the power of the heater [W]; $\Delta\tau$ is the time of heat power supply to the PCM sample during its temperature increasing on Δt [s]; P_{loss} is heat loss [W]; A is the calorimeter heat capacity [J·K^{-1}].

The heat released by the studied PCM sample during its cooling was calculated by the Eq. (3):

$$Q = P_{loss}\Delta\tau - A\Delta t. \quad (3)$$

Specific isobaric effective heat capacity (the heat spent both on

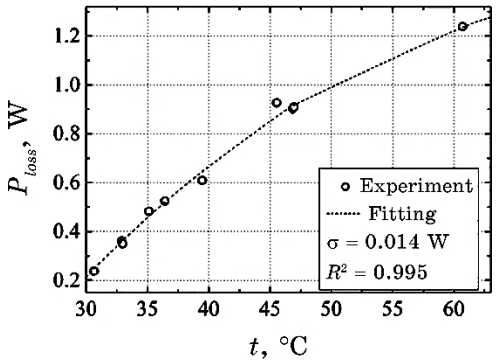

Fig. 3. Dependence of heat loss on the temperature of the measuring cell wall (reading of thermocouple *5*) at the ambient temperature of 28.5 ± ± 0.8°C.

temperature increase and structural changes in the material are considered) of the PCM sample is

$$c_P = \frac{Q}{m\Delta t}, \tag{4}$$

where c_P is the specific isobaric effective heat capacity [$J \cdot g^{-1} \cdot K^{-1}$]; Δt is the PCM sample temperature change during time $\Delta\tau$; m is the mass of the sample [g].

The total enthalpy of solid–liquid phase transition λ_{S-L} is

$$\lambda_{S-L} = \frac{\left(P - P_{loss}\right)\Delta\tau_{S-L} - A\Delta t_{S-L}}{m}, \tag{5}$$

where $\Delta\tau_{S-L}$ is the phase transition duration (obtained from the thermograms) [s]; $\Delta\tau_{S-L}$ is the difference between the temperatures of start and finish of the phase transition.

4. EXPERIMENTAL RESULTS AND DISCUSSION

4.1. Results

One of the obtained in the experiment time dependences of the sample temperature is shown in Fig. 4. The obtained thermograms demonstrate diffuse in time and temperature phase transitions. The presence of the diffuse phase transitions can be explained as follows: the heat supplied to the sample (or released by the sample) during its heating/cooling, can be simultaneously consumed by changing the sample temperature, phase transition or the sample

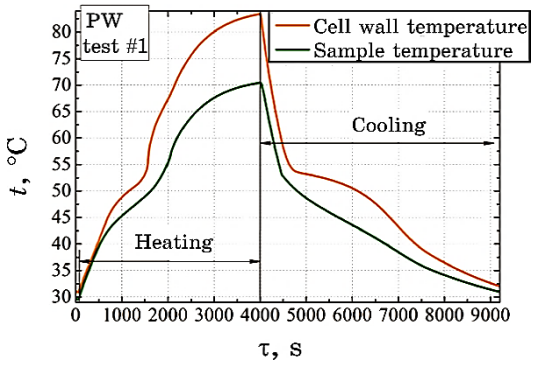

Fig. 4. Time dependence of the PW sample temperature (readings of thermocouple *6*) and the cell wall temperature (the readings of the thermocouple *5*) during the sample heating and cooling.

superheating/supercooling. According to the mentioned reasons, the evaluation of the temperature and total enthalpy of the phase transition using the obtained thermograms was a complex task.

The obtained in experiment time dependences of the samples' temperature were divided into several sections, which have been fitted by a polynomial dependence (with standard deviation σ no more than 0.03 K). The temperature dependences of the specific isobaric effective heat capacity of the PCMs samples were obtained (Fig. 5) using the fitting dependences and Eqs. (1)–(4).

The interpretation of the obtained data is a complex task for the following reasons. Firstly, industrial PW is a mixture of hydrocarbons of different molar masses. Secondly, PW has a heterogeneous solid phase structure (various sizes of crystals and amorphous inclusions). Moreover, solid PW contains dissolved air [13, 14].

Both different melting temperatures of the individual components and endothermicity of deaeration during melting lead to the appearance of the peaks and troughs on the obtained temperature dependences of the specific isobaric heat capacity. These effects are complicated to explain. Given the above, the evaluation of the phase transition total enthalpy instead of the phase transition latent heat is appropriate for the composite PCMs. Moreover, for the determination of the phase transition parameters, it is expedient to use the results of the experiment during the sample's cooling. Herewith, the influence of the main noise factors (the temperatures' field nonuniformity during heating and deaeration influence) is absent.

Obtained from the temperature dependences of the specific effective heat capacity (Fig. 5) parameters (the temperatures of start and finish of the phase transition, the phase transition total enthalpy and specific isobaric heat capacity of the liquid phase in the studied temperature range) are given in Table 1. When the cooling process is considered, the term $P\Delta\tau$ in Eq. (5) is equal to zero and the term $P_{loss}\Delta\tau$ is negative. The value of $P_{loss}\Delta\tau$ was evaluated as an integral in the range from the temperature of the beginning to the temperature of the end of the phase transition of the function $t_5 = f(\tau)$ (Fig. 5). Additionally, to verify the obtained results, the PW latent heat was evaluated (Fig. 6). The experimental latent heat values were compared with references data for PW with close melting point (Table 2). It should be noted that the accurate determination of the temperatures of start and finish of the phase transition by the obtained dependences was complicated. Therefore, the obtained latent heat values for PW are approximate.

4.2. Uncertainty Analysis

The uncertainty analysis of the specific isobaric heat capacity was

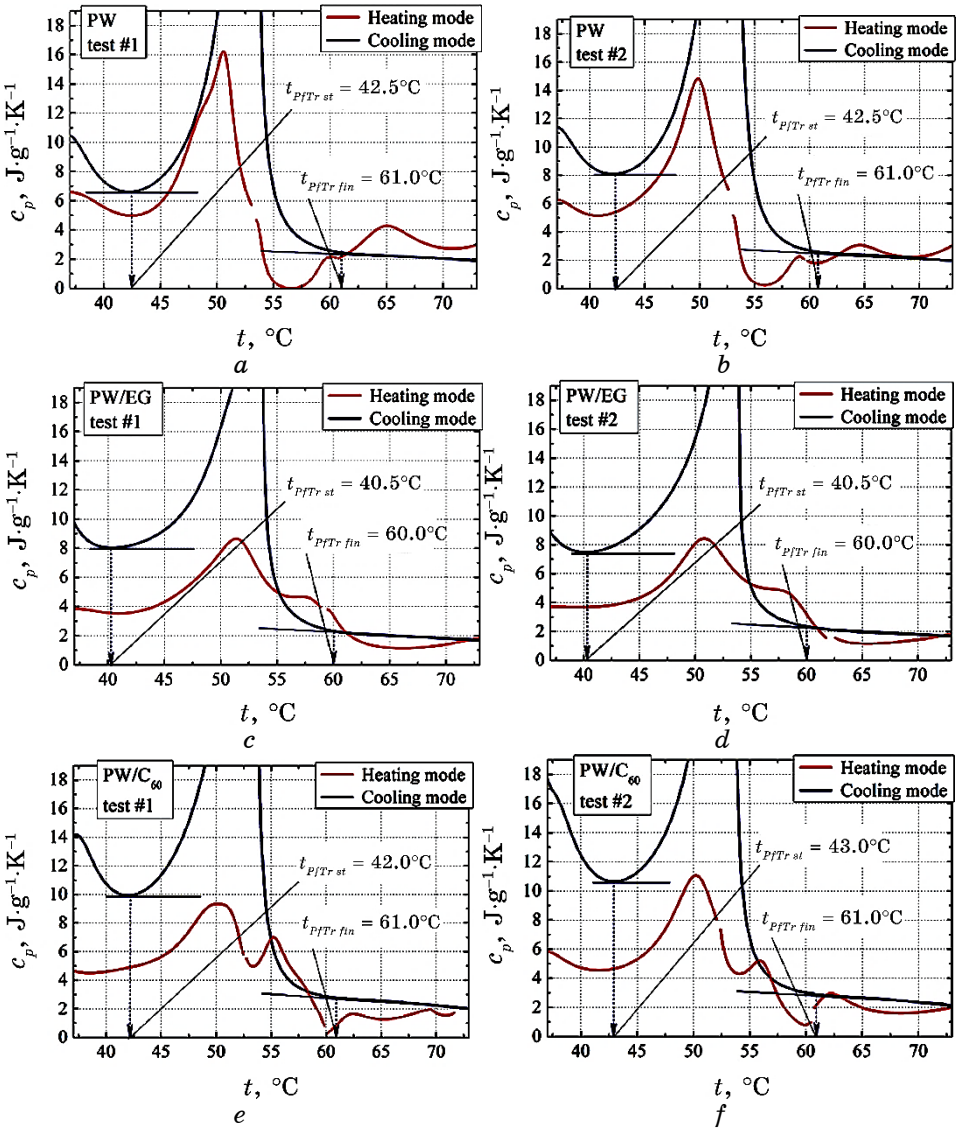

Fig. 5. The temperature dependence of the specific isobaric effective heat capacity for the samples of PW (*a* and *b*), PW/EG (*c* and *d*), and PW/C_{60} (*e* and *f*).

performed according to the recommendations reported by Taylor and Kuyatt [18]. Both components of the uncertainty, namely, type *A* 'random' and type *B* 'systematic', have been considered.

The inputs for the uncertainty evaluation and evaluated maximum combined standard uncertainties are listed in Tables 3 and 4.

TABLE 1. Solid–liquid phase transition parameters for the object of study.

	The total enthalpy of the phase transition			Specific isobaric heat capacity (liquid, 61–70°C), $J \cdot g^{-1} \cdot K^{-1}$
	Starting temperature, °C	Finishing temperature, °C	Specific heat, $J \cdot g^{-1}$	
PW (test 1)	42.5	61.0	256.8	2.22
PW (test 2)			273.4	2.34
PW/EG (test 1)	40.5	60.0	215.5	1.99
PW/EG (test 2)			219.3	1.96
PW/C_{60} (test 1)	42.0–43.0	61.0	293.1	2.52
PW/ C_{60} (test 2)			306.4	2.63

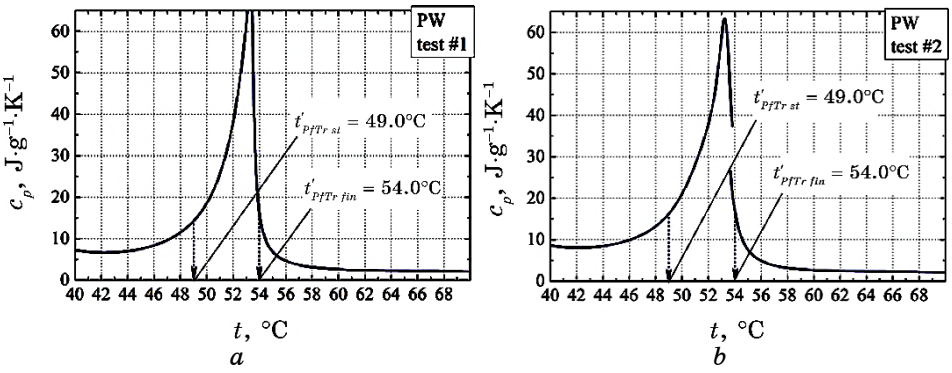

Fig. 6. The temperature dependence of the specific isobaric effective heat capacity for the samples of PW used for evaluation of the phase transition latent heat.

Since the evaluation of the caloric properties was performed for the cooling mode, the uncertainty of the power heater was not taken into account.

4.3. Discussion

The obtained in experiment values of the specific isobaric effective heat capacity of the PW solid phase (Fig. 5, *a*, *b*) are significantly

TABLE 2. The caloric properties of laboratory grade and industrial grade types of paraffin.

Grade	Laboratory grade	Industrial grade
Phase transition latent heat, $J \cdot g^{-1}$	146 $t_{PhTr} = 54{,}4°C$ [15] 194.6 $t_{PhTr} = 41.6°C$ (*n*-docosan) [10]	171–175 $t_{PhTr} = 53.5°C$ (own measurement) 170 average value for all PW [16] 184 $t_{PhTr} = 52–54°C$ (producer Ter Hell Paraffin, Hamburg, FRG) [15] 210 $t_{PhTr} = 45–48°C$ (producer Sun Company, USA) [15] 184.48 $t_{PhTr} = 53°C$ [17] 147–163 $t_{PhTr} = 48–68°C$ [17]
Specific isobaric heat capacity, $J \cdot g^{-1} \cdot K^{-1}$	2.38 (liquid) and 1.93 (solid) $t_{PhTr} = 41.6°C$ (*n*-docosan) [10]	2.2–2.3 (liquid) $t_{PhTr} = 53.5°C$ (own measurement) 2.384 (solid) $t_{PhTr} = 53°C$ [17] 2.981 (liquid, 60–63°C) and 2.604 (solid, 35–40°C) $t_{PhTr} = 48–68°C$ [17]

higher than the references values (Table 2). The presence of the peaks and troughs on the effective heat capacity temperature dependences should be noted. Their presence can be explained both by phase transitions of industrial PW components and by the heat absorption at the deaeration of the moulted PW. Moreover, the amplitude and location of peaks and troughs on the temperature dependencies of the effective heat capacity are different for all objects of study. These effects can indicate that C_{60} and EG in PW differently affect the level of modification of the PW internal structure and the content of dissolved air in PW.

The application of the vacuum glass cover allowed both to observe visually the appearance of gas bubbles in the sample during its melting and to indicate superheating of the sample solid phase during heating above the melting temperature (up to 20°C by thermocouple 6 readings). The C_{60} and EG in PW contributed to a decrease in superheating degree.

The obtained values of the phase transition latent heat and specific isobaric heat capacity of PW liquid phase (Table 1) are in agreement with the references data (Table 2). This result allows performing a comparative analysis of the effect of various CNSs on the caloric properties of composite PCMs using the proposed in this paper experimental setup.

An analysis of Fig. 5 has shown that the EG (0.111 $g \cdot g^{-1}$) in PW contributes to a slight decrease in the temperatures of start and finish of the phase transition (0.5–2.0°C), on the other hand, the presence of C_{60} (0.000936 $g \cdot g^{-1}$) does not affect these parameters.

TABLE 3. Input parameters for uncertainty evaluation.

Parameter	Uncertainty, unit
Mass	0.0005 g
Temperature	0.5 K
Time	0.5 s

TABLE 4. Summary of uncertainty evaluation.

Parameter	Maximum combined standard uncertainty
EG mass fraction	0.001 $g \cdot g^{-1}$
C_{60} mass fraction	0.01 $g \cdot g^{-1}$
Type A uncertainty for heat loss	0.014 W
Calorimeter heat capacity	0.017 $J \cdot K^{-1}$
Difference of temperatures of phase transition start and finish	0.4 K
Released heat	0.2 J
Specific isobaric heat capacity	0.07 $J \cdot g^{-1} \cdot K^{-1}$
Phase transition total enthalpy	6.9 $J \cdot g^{-1}$

The obtained experimental data have shown that the presence of 0.111 $g \cdot g^{-1}$ of EG in PW contributes to a decrease of the phase transition total enthalpy by 15–21%. This effect was expected. In the authors' opinion, this can be explained by the following. Firstly, EG is not involved in the phase change (0.111 $g \cdot g^{-1}$). According to this approach, the total enthalpy of the phase transition of the composite PCM is almost equivalent to the values calculated by multiplying the total enthalpy of pure PW with its mass fraction. This approach is confirmed by the results of some authors. For example, in Ref. [10], it was shown that the latent heat of form-stable EG-based composite PCM saturated with 90 wt.% paraffin is 178.3 $kJ \cdot kg^{-1}$ *vs.* 194.6 $kJ \cdot kg^{-1}$ for pure paraffin. This is close to the results within the approach described above. Secondly, a 'solid-like' structured phase from the molecules of the base fluid near the surface of the solid component can be formed in the composite PCMs in the liquid state. Conceivably, ether this phase has not the structure change or it is needed less heat on structural change during the phase transition. The presence of this phase can contribute to a decrease in the phase transition total enthalpy (its relative values were estimated by the approach mentioned above). At the same time, there are studies with the opposite result. In Ref. [19], it was reported that small content of EG in PW (0.5–1.0 wt.%) leads to an

increase in the melting and freezing latent heats (up to 5% and 7%, respectively) compared to pure PW. When the content of EG increase up to 3.0–4.0 wt.%, the decrease in the latent heat was observed compared to pure PW. The authors of Ref. [19] explained the obtained enhancement by the increase in the PW crystallinity and the strong intermolecular interactions or adhesive work derived from van der Waals force between PW and EG at a small fraction of EG.

The effect of increasing the phase transition total enthalpy by 7–16% at the presence of 0.000936 $g \cdot g^{-1}$ of C_{60} in PW is noteworthy. This effect can be explained by PW's internal structure change around the C_{60} molecules. The effect of C_{60} on the internal structure changes in hydrocarbons was considered in the studies [20–23], in which the solution of fullerenes C_{60} and C_{70} in aromatic hydrocarbons were investigated. In addition, similar results of the effect of a low fraction of CNSs in PW on its phase transition latent heat were obtained in several studies. For example, it is discussed in the previously mentioned study [19]. In addition, in Ref. [24], it was established 6.3%-higher enthalpy of phase change for MWCNT (0.5% wt.)/paraffin nanocomposite vs pure paraffin. The obtained effect in Ref. [24] was explained by the more rapid nucleation of larger crystallites by MWCNTs proceeding via short- and long-range templating as well as intrinsic characteristics of MWCNTs.

A qualitatively similar effect of C_{60} and EG was observed for the specific isobaric heat capacity of the liquid phase of the objects of study: the presence of 0.111 $g \cdot g^{-1}$ of EG in PW contributed to the heat capacity decreasing by 10–16%, while the presence of 0.000936 $g \cdot g^{-1}$ of C_{60}, to the heat capacity increasing by 7–15%.

The obtained quantitative results require more accurate further measurements to confirm them and to clarify the physical effects. The confirmation of the obtained effects for PCM PW/C_{60} is an important step for their introduction in the industry since an increase in the phase transition total enthalpy of PCM will allow to increase the efficiency of TES systems and to reduce their mass and size. Further studying of PCM PW/EG is important to find a rational content of EG. The reasonable content of EG can significantly increase the thermal conductivity of PCM, which will improve the efficiency of TES systems.

5. CONCLUSION

The experimental setup of a new design for measuring the composite PCMs caloric properties was created. Setup advantages are the simple design, low cost (compared to adiabatic calorimeter or differential scanning calorimeter), and visualization of the sample dur-

ing the experiment. The setup applying is appropriate for estimation of expediency of further studying of composite PCMs.

It was shown that the EG content (0.111 $g \cdot g^{-1}$) in PW (melting point 53.5°C) contributes to a slight decrease in the temperatures of start and finish of the phase transition (0.5–2.0°C), on the other hand, the presence of C_{60} (0.000936 $g \cdot g^{-1}$) does not affect this parameter. The phase transition total enthalpy for PW/EG was 15–21% less and for PW/C_{60} was 7–16% higher than for pure PW. A qualitatively similar effects of C_{60} and EG were observed for the specific isobaric heat capacity of the liquid phase of the objects of study: the EG contributed to decreasing the heat capacity of PW by 10–16%; oppositely, C_{60} presence in PW increases its heat capacity by 7–15%. The obtained effects can be explained by both presences of the CNSs themselves, and structural changes in the PW caused by CNSs.

The expediency of further studies of composite PCMs from PW/CNSs to confirm the obtained effects for PW/C_{60} and to find a rational fraction of EG in PW/EG was proven.

ACKNOWLEDGMENT

The authors are grateful to the National Research Foundation of Ukraine (project No. 2020.02/0125) for financial support of this study.

REFERENCES

1. K. Faraj, M. Khaled, J. Faraj, F. Hachem, and C. Castelain, *J. Energy Storage*, **33**: 101913 (2021); https://doi.org/10.1016/j.est.2020.101913
2. P. K. S. Rathore and S. K. Shukla, *Renewable Energy*, **176**: 295 (2021); https://doi.org/10.1016/j.renene.2021.05.068
3. O. Khliyeva, V. Zhelezny, A. Paskal, Ya. Hlek, and D. Ivchenko, *East.-Eur. J. Enterp. Technol.*, **4**, No. 5 (112): 12 (2021); https://doi.org/10.15587/1729-4061.2021.239065
4. O. Khliyeva, V. Zhelezny, A. Nikulin, M. Lapardin, D. Ivchenko, and E. Palomo del Barrio, *Proc. 11th Int. Conf. 'Nanomaterials: Applications & Properties' (September 5–11, 2021, Odesa, Ukraine)*, TPNS04-2; https://doi.org/10.1109/NAP51885.2021.9568522
5. N. O. Mchedlov-Petrossyan, *Chemical Reviews*, **113**, No. 7: 5149 (2013); https://doi.org/10.1021/cr3005026
6. Y. Zhao, L. Jin, B. Zou, G. Qiao, T. Zhang, L. Cong, F. Jiang, C. Li, Y. Huang, and Y. Ding, *Appl. Therm. Eng.*, **171**: 115015 (2020); https://doi.org/10.1016/j.applthermaleng.2020.115015
7. X. L. Wang, B. Li, Z. G. Qu, J. F. Zhang, and Z. G. Jin, *Int. J. Heat Mass Transfer*, **155**: 119853 (2020); https://doi.org/10.1016/j.ijheatmasstransfer.2020.119853

8. C. Li, B. Zhang, and Q. Liu, *J. Energy Storage*, **29**: 101339 (2020); https://doi.org/10.1016/j.est.2020.101339
9. M. Kenisarin, K. Mahkamov, F. Kahwash, and I. Makhkamova, *Sol. Energy Mater. Sol. Cells*, **200**: 110026 (2019); https://doi.org/10.1016/j.solmat.2019.110026
10. A. Sari and A. Karaipekli, *Appl. Therm. Eng.*, **27**, Iss. 8–9: 1271 (2007); https://doi.org/10.1016/j.applthermaleng.2006.11.004
11. Y. Grosu, Y. Zhao, A. Giacomello, S. Meloni, J. L. Dauvergne, A. Nikulin, E. Palomo, D. Yulong, and A. Faik, *Appl. Energy*, **269**: 115088 (2020); doi.org/10.1016/j.apenergy.2020.115088
12. R. S. Ruoff, D. S. Tse, R. Malhotra, and D. C. Lorents, *J. Phys. Chem.*, **97**: 3379 (1993); https://doi.org/10.1021/j100115a049
13. L. Klintberg, M. Svedberg, F. Nikolajeff, and G. Thornell, *Sens. Actuators A*, **103**, Iss. 3: 307 (2003); https://doi.org/10.1016/S0924-4247(02)00403-X
14. J. DeSain, B. Brady, K. Metzler, and T. Curtiss, *Proc. 45th AIAA/ASME/SAE/ASEE Joint Propulsion Conf. & Exhibit (August, 2009, Denver, Colorado)*, AIAA 2009-5115; https://doi.org/10.2514/6.2009-5115
15. A. Sharma, S. D. Sharma, and D. Buddhi, *Energy Convers. Manage.*, **14**: 1923 (2002); https://doi.org/10.1016/S0196-8904(01)00131-5
16. M. Freund, R. Csicos, S. Keszthelyi, and G. Y. Mozes, *Paraffin Products: Properties, Technologies, Applications* (Amsterdam: Elsevier: 1982), p. 335.
17. N. Ukrainczyk, S. Kurajica, and J. Šipušić, *Chem. Biochem. Eng. Q*, **24**, No. 2: 129 (2010).
18. B. N. Taylor and C. E. Kuyatt, *Guidelines for Evaluating and Expressing the Uncertainty of NIST Measurement Results. NIST Technical Note 1297 1994 Edition* (Washington: NIST: 1994), p. 20.
19. G. Fang, M. Yu, K. Meng, F. Shang, and X. Tan, *Energy & Fuels*, **34**, No. 8: 10109 (2020); https://doi.org/10.1021/acs.energyfuels.0c00955
20. B. M. Ginzburg, S. Tuichiev, and S. K. Tabarov, *J. Macromol. Sci. Part B: Phys.*, **52**, Iss. 6: 773 (2013); https://doi.org/10.1080/00222348.2012.721654
21. B. M. Ginzburg, S. Tuichiev, D. Rashidov, F. H. Sodikov, S. H. Tabarov, and A. A. Shepelevskii, *J. Macromol. Sci. Part B: Phys.*, **54**, Iss. 5: 533 (2015); https://doi.org/10.1080/00222348.2015.1010635
22. V. P. Zhelezny, K. Y. Khanchych, I. V. Motovoy, and A. S. Nikulina, *J. Mol. Liq.*, **328**: 115416 (2021); https://doi.org/10.1016/j.molliq.2021.115416
23. V. P. Zhelezny, K. Y. Khanchych, I. V. Motovoy, and A. S. Nikulina, *J. Mol. Liq.*, **338**: 116629 (2021); https://doi.org/10.1016/j.molliq.2021.116629
24. A. W. Kuziel, G. Dzido, R. Turczyn, R. G. Jędrysiak, A. Kolanowska, A. Tracz, W. Zieba, A. Cyganiuk, A. P. Terzyk, and S. Boncel, *J. Energy Storage*, **36**: 102396 (2021); https://doi.org/10.1016/j.est.2021.102396